International Journal of Pharmaceutics 616 (2022) 121505

Contents lists available at ScienceDirect

International Journal of Pharmaceutics

journal homepage: www.elsevier.com/locate/ijpharm

Mefenamic acid solid dispersions: Impact of formulation composition on processing parameters, product properties and performance

Elke Prasad *, John Robertson, Gavin W. Halbert

EPSRC Future Manufacturing Research Hub in Continuous Manufacturing and Advanced Crystallisation, University of Strathclyde, Technology and Innovation Centre, 99 George Street, Glasgow G1 1RD, UK
Strathclyde Institute for Pharmacy and Biomedical Sciences, University of Strathclyde, 161 Cathedral Street, Glasgow G4 0RE, UK

ARTICLE INFO

Keywords:
Extrusion
Solid dosage form
Oral drug delivery
Solid dispersion
Dissolution
Formulation

ABSTRACT

The objective of this study was to develop an immediate release (IR), crystalline solid dispersion (CSD) formulation of Mefenamic acid (MFA) by hot-melt-extrusion (HME) and assess the impact of drug loading on process parameters, product physico-chemical properties and product performance. An HME process to produce a range of MFA-Soluplus®-Sorbitol polymer matrix CSD formulations was developed based on rheological screening assays of physical mixtures (PM). The impact of drug loading on process parameters was compared to the impact of drug loading on the physico-chemical properties of formulations. Based on process and product data, three groupings of API drug loading were identified: sub-saturated, saturated, and supersaturated systems. CSD formulations were obtained for 20–50% (w/w) drug loading containing the stable polymorphic form I of MFA. CSD formulations predominantly improved the consistency of the product performance. An Amorphous Solid Dispersion (ASD) was obtained for 10% (w/w) drug loading, exhibiting faster drug release even at physiologically relevant pH. This study illustrates the impact of drug loading on process and product characteristics and how a better understanding of maximum API solubility in a given polymer system can improve targeted formulation development.

1. Introduction

Mefenamic acid is a nonsteroidal anti-inflammatory drug and is used to treat mild to moderate pain. MFA is classed as a BCS class IIa drug (Butler and Dressman, 2010; Nurhikmah et al., 2016), showing poor solubility and high permeability, but also dissolution rate limited (Butler and Dressman, 2010) absorption of the drug into the body. For dissolution rate limited drugs, formulation approaches carefully need to consider the polymorphic form (Romero et al., 1999), particle size, surface area and wettability of the drug to achieve complete oral absorption (Butler and Dressman, 2010; Vasconcelos et al., 2007). Three crystalline forms have been published for MFA, with form I the most stable at ambient temperature (Surov et al., 2009). Form II and III are metastable states (Abdul Mudalip et al., 2013). Upon heating MFA form I, phase transition of the stable form can occur via sublimation (Brittain, 2016; SeethaLekshmi and Guru Row, 2012; Surov et al., 2009).

MFA drug product is available on the market as a powder filled capsule formulation (250 mg) and as a tablet formulation (500 mg). A range of formulation approaches intending to improve the low solubility and inconsistent bioavailability of MFA have been reported. These ranged from dry milling (particle size reduction and increase in amorphous content) (Hummel and Buchmann, 2000), micellar solutions (Ullah et al., 2014), β-cyclodextrin complexes (Derle et al., 2008), self-emulsifying drug-delivery systems (SEDDS (Gursoy and Benita, 2004) and SMEDDS (Kumar et al., 2019; Sriamornsak et al., 2015)) to solid dispersions (Alshehri et al., 2015; Andrews et al., 2009; Darwich, 2015; Prasad et al., 2020; Rao et al., 2011).

Solid dispersions offer the possibility to accommodate a range of approaches to improve the oral bioavailability of poorly water-soluble drugs. The excipients (polymer matrix carrier) can contain the drug in crystalline form, amorphous form, or can be molecularly dispersed (Tambosi et al., 2018). In this type of system, the drug particle size can be reduced to the complete minimum, and the close interaction of polymer matrix with the drug molecule can highly increase wettability and, in turn, bioavailability may be significantly improved (Rao et al., 2011; Vasconcelos et al., 2007). A variety of methods, such as the melt

Abbreviations: PM, physical mixture; EX, extrudate; MFA, Mefenamic acid.

* Corresponding author.
E-mail address: elke.prasad@strath.ac.uk (E. Prasad).

https://doi.org/10.1016/j.ijpharm.2022.121505
Received 2 December 2021; Received in revised form 19 January 2022; Accepted 20 January 2022
Available online 24 January 2022

method (Andrews et al., 2009; Owusu-Ababio et al., 1998), solvent evaporation method (Rao et al., 2011) and hot melt extrusion (Alshehri et al., 2015; Darwich, 2015; Prasad et al., 2020) have been employed to prepare solid dispersions with MFA as the active ingredient.

A range of different classes of polymer systems have been investigated to formulate MFA into solid dispersions: polyoxyethylene-polypropylene (Lutrol F68) (Andrews et al., 2009), binary and ternary systems based on polyvinylpyrrolidone (PVP) and a sodium starch glycolate super disintegrant (Primojel®) (Rao et al., 2011), as well as binary and ternary mixtures of polyethylene glycol (PEG 3350) and polysorbate 20 (Tween 20) (Owusu-Ababio et al., 1998). HME based studies investigated the use of a dimethylaminoethyl methacrylate-copolymer (Alshehri et al., 2015) (Eudragit® E PO) and polyvinyl caprolactam-polyvinyl acetate-polyethylene glycol graft copolymer (Darwich, 2015; Prasad et al., 2020) (Soluplus®) and combinations thereof (Darwich, 2015) to prepare solid dispersions.

Solid dispersions prepared by hot melt extrusion can achieve higher amorphous drug loadings compared to other methods. In case of MFA and Eudragit® E PO a maximum of 33% w/w amorphous drug loadings (was achieved (Darwich, 2015). This is not surprising since the cationic amine groups of Eudragit® E PO facilitate and aid dissolution of MFA in the polymer due to ionic interactions. However, the cationic groups also give rise to pH dependant drug release from this polymer matrix (Alshehri et al., 2015; Darwich, 2015). This is not the case for the non-ionic Soluplus® polymer, making it a suitable vehicle for an immediate release platform (Prasad et al., 2020). Amorphous solid dispersions (ASD) exhibit higher internal energy than crystalline solid dispersions (CSD) (Zografi and Newman, 2017), which is seen as significant improvement of their aqueous solubility. However, this can also provide a thermodynamic driving force for phase separation and crystallisation (Bordos et al., 2019). This can give rise to stability studies of the amorphous formulations failing to meet product specification regarding their product performance.

In order to avoid potential physical stability issues of ASDs, a recent study formulated an IR dose form with MFA in Soluplus® as a crystalline solid dispersion (CSD) (Prasad et al., 2020). The polymer matrix was plasticised with 15% w/w Sorbitol in order to reduce the HME process temperature to retain the crystalline nature and stable polymorphic form I of MFA. The formulation showed improved consistency in drug release compared to commercial capsules (Prasad et al., 2020).

In this study the impact of drug loading on process and formulation development of CSDs containing MFA is presented. The aim of the study was to produce CSDs of a range of Mefenamic acid - polymer matrix (SOL15: 85% w/w Soluplus®, 15% w/w Sorbitol) formulations in order to investigate and better understand the effect of drug loading on HME process parameters and the relationship to physico-chemical properties of extrudates and their product performance.

This work forms part of the broader aim of the EPSRC Future Manufacturing Research HUB at CMAC. The project aims to implement integrated continuous, laboratory scale manufacturing platforms by the means of crystal engineering of a model drug (MFA), coupled with polymer processing steps to deliver enhanced physical properties for biopharmaceutics performance.

2. Materials and methods

2.1. Materials

Soluplus® polymer was obtained as free sample from BASF (Ludwigshafen, Germany). Tris(hydroxymethyl)aminomethane (Tris), Sorbitol Emprove Parteck SI 150, Sodium dodecyl sulphate Ph Eur (SDS), Mefenamic acid (MFA), and Trifluoroacetic acid (TFA) were obtained from Sigma Aldrich (Gillingham, UK). CR UK Formulation unit (University of Strathclyde, UK), donated hard gelatine capsules, Licap® size 0, Phosphoric acid 85% for HPLC, Ethanol absolute, Hydrochloric acid and Sodium hydroxide were obtained from VWR (Lutterworth, UK).

2.2. Mefenamic acid form II

MFA form I was added to N, N-di-methyl formamide at a concentration of 200 mg/g. The mixture was stirred at 400 rpm and 65 °C until fully dissolved. Once fully dissolved, the solution was cooled in a −20 °C freezer with form II crystallising upon cooling. The crystals were then filtered and dried over night at 65 °C. MFA form II was used as a reference in FTIR measurements.

2.3. Formulations

Formulations were prepared by initially passing powders through a 1 mm mesh sieve prior to weighing. Powders were weighed and then blended in a Pharmatech Bin blender AB-015. The bin blender was equipped with a 5 L vessel for larger (~500 g) samples or a 1 L vessel for smaller (~200 g) samples. The blender was set to mix for 10 mins with 17 rpm and an agitator speed of 100 rpm. Powder blends containing 0 – 40 % w/w Mefenamic acid in a Soluplus® polymer matrix containing 15 % (w/w) Sorbitol were prepared (Table 1).

2.4. Rheology

Physical mixtures (PM) of formulations were analysed on a rotational rheometer (Haake Mars III, Thermo Fisher, Karlsruhe) equipped with a 25 mm diameter parallel plate geometry (Prasad et al., 2020). 500 mg of powdered sample were compressed under vacuum at 2 tonnes for 2 min using a manual hydraulic press. The resulting discs were 25 mm in diameter. Extrudate samples, were pelletised prior to analysis. 500 mg of extrudates were carefully added to the measurement geometry to fully cover the plate geometry. Prior to analysis, zero gap height calibrations were performed. Measurements were performed in the linear visco-elastic region (LVR) of materials.

Oscillatory temperature sweep – PMs: Sample discs were loaded and equilibrated for 5 min. Temperature sweeps were performed from high (160 °C) to low (110 °C) temperature, with a constant deformation of 0.5 %. Measurements were recorded at a frequency of 1 Hz. A normal force of 0.1 N was employed to control the gap of the plate geometry. Temperature sweeps for extrudates were performed from low (110 °C) to high (160 °C) temperature.

Oscillatory frequency sweeps – Physical mixtures: Sample discs were allowed to equilibrate to temperature for 2 mins prior to analysis. The test temperature for frequency sweeps encompassed 120 °C, 130 °C and 140 °C. The deformation was kept constant at 0.5 % across a frequency range from 0.1 − 100 Hz.

2.5. Hot-Melt-Extrusion

Hot melt extrusion of formulations was performed on a Process 11 (Thermo Fisher, Karlsruhe, Germany) twin screw extruder as previously reported (Prasad et al., 2020). The extruder was set up with a 1.6 mm round die and a screw configuration of:14 feed screws − 6 × 60°F bilobe mixing elements − 7 × feed screws – 3 × 30° F, 3 × 60° F, 4 × 90° bilobe mixing elements – 13 feed screws - discharge element. A 2000 Series melt pressure transducer (Terwin Instruments Ltd, Bottesford, UK) was used to monitor the pressure in the die of the extruder. A Brabender LIW

Table 1
Mefenamic acid formulation composition.

Formulation	D-Sorbitol (% w/w)	Soluplus® (% w/w)
SOL15	15	85
Formulation	Mefenamic acid (% w/w)	SOL15 (% w/w)
10MFA	10	90
20MFA	20	80
30MFA	30	70
40MFA	40	60
50MFA	50	50

feeder machine (type DDW-N-MT) with twin concave screws (TC12/12) (Brabender, Duisburg, Germany) was calibrated for maximum output prior to HME studies. The % of maximum torque was reported based on the upper Torque limit of the Process 11 (12 Nm). The specific mechanical energy consumption (SMEC) was calculated based on the following relationship:

$$SMEC\left[\frac{kJ}{kg}\right] = \left(\frac{Torque[Nm]}{1000}\right) * \left(\frac{screwspeed[rpm]}{feedrate\left[\frac{kg}{min}\right]}\right) \quad (1)$$

2.6. Differential scanning calorimetry (DSC)

DSC analysis of powdered and extruded formulations was performed on a DSC214 Polyma, Netzsch (Selb, Germany). Samples were presented in 25 μL Aluminium crucibles with a sealed, pierced lid. Extruded filaments were hand cut and 5–10 mg analysed at 20 °C/min heating rate from 0 to 250 °C. The system used Helium purge gas at 40 mL/min and Helium protective gas at 60 mL/min.

2.7. FTIR

PMs and extruded filaments were analysed on a Bruker Tensor II equipped with a Platinum ATR accessory. Sample analysis was performed with 16 scans at a resolution of resolution 2 cm^{-1}. The recorded signal covered wavenumber 4000 to 400 cm^{-1}.

2.8. Mechanical testing

Mechanical properties of filaments were tested on a Texture Analyser TA-XT equipped with a mini 3-point bend rig (Prasad et al., 2019). Briefly, five replicates of extruded filaments were tested with the following settings: gap 0.8 cm, upper blade speed blade speed 0.02 mm/sec and a total displacement of 4.5 mm. Exponent software (version 6.1.11.0) was used to acquire data, as well as data analysis.

The Flexural modulus was determined as the slope of the stress strain graph. The maximum stress and strain at maximum stress were also determined. The break point was associated with the minima in the first derivative of the stress data. Stress at break and Strain at break values were also reported. The modulus of toughness was reported as the area under the curve to the break point.

2.9. SEM

Extruded filaments were hand cut to pellets and added to aluminium stubs with sticky carbon tabs. The side of the extruded filament and the cut face were analysed. To reduce charging in the SEM, samples were sputter coated with 20 nm gold layer. Prior to analysis, a vacuum was applied for 2 min. The samples were then transferred to the SEM for analysis using a TM4000Plus SEM (Hitchi, Tokyo, Japan). A beam voltage of 10000 eV with a probe current setting of 2, standard vacuum level (M) was applied, and data collected in backscattered electron mode. Magnifications of 30x, and 2000x were applied.

2.10. XRPD

XRPD data was collected on a Bruker D8 Advance II diffractometer (Bruker, Germany) with the following experimental setup: For crystalline form identification, a small quantity (10–50 mg) of sample was analysed using transmission XRPD data collected on a Bruker AXS D8 Advance transmission diffractometer equipped with θ/θ geometry, with primary monochromated radiation (Cu Kα1 λ = 1.54056 Å), a Vantec PSD and an automated multiposition x-y sample stage. Samples were mounted on a 28-position sample plate supported on a polyimide (Kapton, 7.5 μm thickness) film. Data were collected from each sample in the range 4 − 35° 2θ with a 0.015° 2θ step size and 1 s per step count time. Samples were oscillated in the x-y plane at a speed of 0.3 mm s^{-1} throughout data collection to maximise particle sampling and minimise preferred orientation effects.

2.11. Content analysis - HPLC

Content analysis was performed by HPLC (Prasad et al., 2020). Briefly, analysis was carried out on a reversed phase C-18 stationary phase (Kinetex2.6u C18 50x3 mm) using UV detection and quantification at 278 nm wavelength. A validated gradient method with an aqueous mobile phase (MP) of 0.5 % TFA in dH_20 and organic MP of 0.5 % TFA in HPLC grade Acetonitrile was used. An injection volume of 10 μL was used and samples analysed at 30 °C with a flow rate of 1.47 mL/min. System suitability test and bracketing standards were performed to ensure the validity of the analysis. The analysis was valid across an MFA concentration range from 50 − 300 μg/mL, with a linearity of r^2 = 0.9997 and recovery values of < 2%.

2.12. Performance screening – Inform

Product performance screening was performed on the Sirius Inform instrument (Pion, UK). GI dissolution assays (Gravestock et al., 2011) are small volume (40 mL) dissolution assays. An acetate phosphate buffer was used to allow pH adjustment over a wide pH range, exposing the sample to a total of 4 pH steps (pH 2, 6.5, 7.4, 9) for 30 min each. Sample quantification was based on the UV absorbance spectrum collected online by a fibre optic dip probe with a 10 mm path length in the dissolution medium. UV calibration was performed prior to analysis to determine the molar extinction coefficient (MEC) of Mefenamic across the investigated pH range. pH adjustments were performed with 0.5 M NaOH and 0.5 M HCl, respectively.

Extrudate samples, 10 − 50MFA filaments, were presented as hand cut pellets, approximately 1–4 mm length and filament diameters ranging from ~ 2–2.7 mm. PMs were presented as powder samples. Sample weights equivalent to 5 mg of MFA were added to each vial and the drug release measured over time and the given pH range.

2.13. Drug release testing USP37

Dissolution testing was performed using an ADT8i Dissolution bath (USP I, basket) apparatus with a closed loop setting and a T70 + UV/Visible Spectrophotometer (Automated Lab Systems, Wokingham, UK). A volume of 1000 mL 0.05 M Tris dissolution buffer pH 9 (USP 37 Mefenamic acid capsules) was employed with a basket rotation speed of 100 rpm and a temperature of 37 ± 0.5 °C. Samples were drawn through an 0.2 μm filter before UV analysis was carried out. UV readings at 286 nm (1 mm pathlength) were taken at 5 min intervals. The impact of the presence of excipients was assessed and the analysis deemed valid over an MFA concentration range of 100–300 μg/mL. with a linearity of r^2 = 0.9996 and recovery values of 97.5–105.6%.

Hard gelatine capsules (Licaps®, size 0) were filled with 250 mg Mefenamic acid (Sigma). The PM of 50MFA was filled into hard gelatine capsules (Licaps®, size 0) with fill weights equivalent to 250 mg MFA. Capsules (n = 6) were tested and the '% release normalised to fill weight' reported.

3. Results and discussion

3.1. Powder blend and extrudate content

The theoretical powder blend composition was in good agreement with the determined API content (Table 2). MFA content for extrudates was 2.3 – 3.6 % lower than the PMs. The loss in MFA at elevated temperatures was possibly due to the phase transition of MFA via sublimation (Brittain, 2016; SeethaLekshmi and Guru Row, 2012) (via the

Table 2
MFA content of MFA PMs and extrudates.

	PM % w/w MFA	Extrudate % w/w MFA	% w/w Loss MFA
10MFA	10.5	8.1	2.3
20MFA	19.7	17.3	2.5
30MFA	30.0	26.4	3.6
40MFA	39.1	36.2	2.9

HME vent and from the hot extrudate exiting the die). A loss of 2 % has previously been reported for the 50% w/w MFA formulation (Prasad et al., 2020).

3.2. Rheology - physical mixtures

Targeting a CSD formulation, the lowest extrusion temperature was sought. Temperature sweeps of PMs were performed and form the basis for the selection of suitable HME processing temperature. The oscillatory temperature sweep data of Soluplus® and Soluplus® containing 15% w/w D-Sorbitol as a plasticiser has previously been reported, predicting the lowest extrusion temperature of the plasticised system at 134 °C (Prasad et al., 2020).

The addition of 10 and 20% w/w MFA to the polymer matrix showed complex viscosity similar to the plasticised polymer matrix only (1.7 * 10^3 Pas at 160 °C to 2.4 * 10^5 Pas at 110 °C). This may be due to the low solubility of the lipophilic MFA in the hydrophilic polymer. A further increase in MFA to concentrations ≥ 30% w/w saw poor reproducibility of the temperature sweep data. This behaviour was similar to a 50% w/w mixture investigated by Prasad et al, attributing the behaviour to the sample going through the temperature sweep as a multiphase system, with the pre-measurement temperature equilibration step not sufficiently facilitating MFA dissolution in the polymer and poor sample adhesion to the parallel plate geometry (Prasad et al., 2020).

Complex viscosity values of 8 * 10^2 to 10^4 Pas have been reported as suitable for extrusion on small scale extruders (Kolter et al., 2012). At 132 °C the complex viscosity of 10MFA and 20MFA were close to 10^4 Pas, the upper limit of the ideal viscosity for processing on small scale extruders, and therefore signified the lowest possible processing temperature.

Properties of polymers, as macromolecular molecules, lie between the properties of elastic solids and viscous fluids (Aho et al., 2015). The deformation of polymers, application of stress and the resulting strain in the macromolecular network, are time dependant. Rheological measurements allow to determine the different contributions of elastic and viscous behaviour when stress is applied to a polymer system. The energy stored in materials upon deformation is the Elastic / storage modulus (G'). The energy that is lost via dissipation is the Viscous / loss modulus (G"). The viscous properties of a polymer dominate, when the ratio of G" / G' (tan delta (δ)) > 1, where the polymer system is amenable to movement or flow, desirable for HME application. When tan delta values < 1, the elastic behaviour dictates the overall behaviour and may cause difficulties during extrusion.

Frequency sweeps were performed at temperatures (120, 130 and 140 °C) close to the lowest predicted processing temperature. An inverse relationship of complex viscosity and angular frequency was observed for all PMs, signifying the shear thinning behaviour of the system (20MFA data - Fig. 1A).

Viscous behaviour of PMs dominated across the lower frequency ranges, seen as high tan delta values ranging from 4.2 at 140 °C to 2.8 at 120 °C (Fig. 1B). With increasing angular frequencies, a decrease in tan delta values was observed. This was due to an increase in storage modulus to similar levels as the loss modulus. The increase in elastic contribution to the overall behaviour of the polymer with shear may be seen as an increase in die swell during the extrusion process.

Based on the complex viscosity results (shear thinning as well as viscoelastic behaviour of MFA PMs) and the desire to reduce the process temperature to a minimum in order to retain MFA form I, a compromise in the process temperature was sought to enable processing on a small-scale extruder. Although the observed shear thinning behaviour may allow processing at lower temperatures, low screw speed and feed rate was sought to allow for slow post processing steps. Based on these findings and considerations, the starting point for HME processing trials for MFA containing formulations was 140 °C, aiming for subsequent stepwise reduction in process temperature to identify the lowest possible extrusion temperature. Due to the higher complex viscosity of Soluplus®, HME trials for polymer samples only were started at 160 °C.

3.3. HME results

3.3.1. Impact of drug loading on lowest extrusion temperature (at fixed feed rate and screw speed)

An initial process temperature of 140 °C, followed by a stepwise reduction was targeted, in order to identify the lowest possible extrusion temperature. HME process data for SOL15 and 50MFA have previously been reported (Prasad et al., 2020) and are included for comparison. The powder feed rate and screw speed for HME experiments were kept constant for initial HME trials at 0.1 kg/h and 50 rpm, respectively. The lowest processing temperature for neat polymer was identified as 150 °C. This was in good agreement with the results previously obtained from the oscillatory temperature sweep (Prasad et al., 2020). The plasticised polymer (SOL15) had previously been assessed for the lowest processing temperature at 130 °C (Prasad et al., 2020).

The lowest processing temperatures at 50 rpm were 120 °C for 20MFA and 30MFA formulations and 125 °C for the 10MFA, 40MFA and

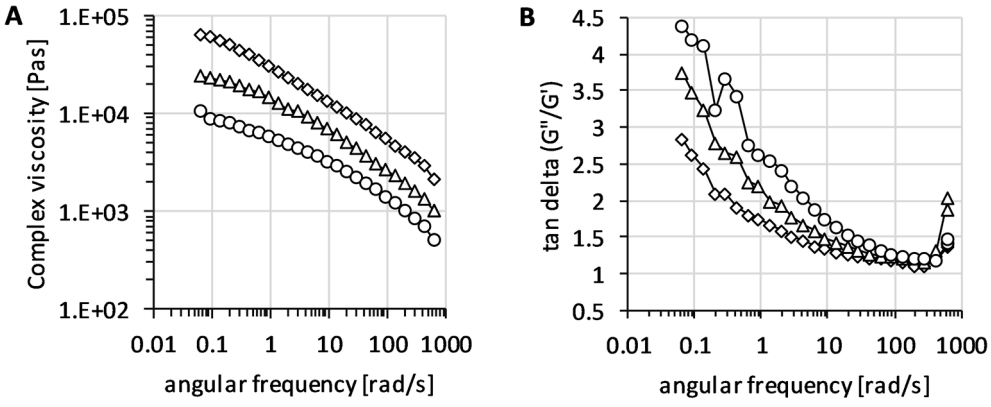

Fig. 1. Oscillatory frequency sweep of 20MFA PM: (A) complex viscosity and (B) tan delta (Loss modulus G" / Storage modulus G') versus angular frequency: diamond – 120 °C, triangle – 130 °C, square – 140 °C (n = 2).

50MFA formulation. 10MFA extrudate was clear in appearance, whilst 20 – 40MFA extrudates were white in appearance (Fig. 2). This was indicative of the presence of crystalline MFA, as previously reported for the 50MFA formulation (Prasad et al., 2020).

HME process data from the extrusion of SOL15 and 0 – 50 % w/w MFA is shown in Fig. 3. With the addition of MFA to the polymer matrix, a reduction in torque was observed signifying a plasticisation effect of MFA in the polymer matrix. This was concomitant with an increase in die pressure with drug loadings, reaching a maximum at 20 % w/w. Drug loadings > 20 % w/w saw a decrease in die pressure. A one-way ANOVA test with Tukey pairwise comparison showed no shared mean for torque values of all formulations but a shared mean for die pressure of the 40 and 50% w/w MFA formulations (Table S 1, Table S 2). The product temperature across all compositions was consistently 4–5 °C lower than the die temperature.

The specific mechanical energy consumption (SMEC) for the polymer matrix only was decreased when MFA was added to the formulation. A maximum reduction was achieved at ≥ 20% w/w drug loading. However, the initial reduction in SMEC from 0 to 10% w/w drug loading was larger than the 10 to 20% w/w reduction (Fig. 4, Table S 3).

Die swell was observed for all formulations (Fig. 5, Table S 4). The filament diameter of extrudates followed a similar trend to the die pressure profile during extrusion: 10 and 20% w/w drug loading saw an increase in die swell ratio of up to a maximum of 1.7. With less polymer available in the 40 and 50 % w/w formulation, die swell behaviour similar to the polymer matrix with a ratio of only 1.3 was observed.

3.3.2. *Impact of screw speed on process parameters (at fixed feed rate)*

Data for SOL15 and 50MFA have previously been reported (Prasad et al., 2020) and are included in the results for comparison. Neat polymer and the plasticised polymer (SOL15) showed shear thinning behaviour, seen as a decrease in torque with increasing screw speed (Prasad et al., 2020). This effect was not as strong for formulations containing MFA (Fig. 6). No significant impact of screw speed on die pressure was observed for Soluplus® and SOL15. Formulations containing MFA showed a decrease in die pressure in relation to screw speed.

3.4. *Differential scanning calorimetry*

DSC analysis of MFA powder was in good agreement with MFA form I

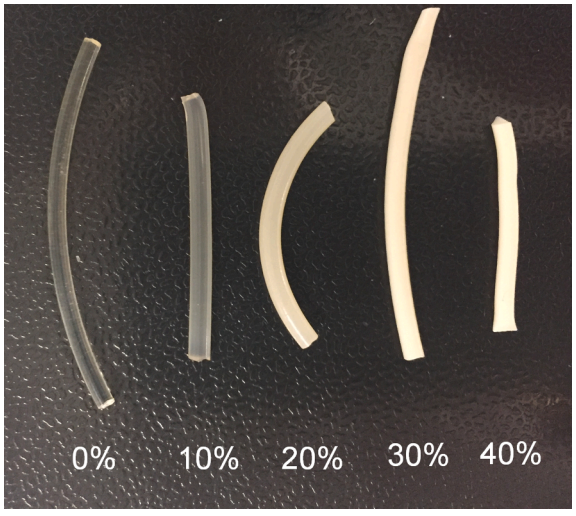

Fig. 2. Filament extrudates (from left to right): SOL15 (0) – 10–20 – 30–40 MFA (0.1 kg/h feed rate, 50 rpm, process temperatures SOL15 – 130°, 10/40/50MFA – 125 °C, 20 and 30MFA – 120 °C). Filament diameter from left to right: 2.10, 2.49, 2.70, 2.41, 2.21, 2.08 mm (n = 3). SOL15 extrudate from (Prasad et al., 2020).

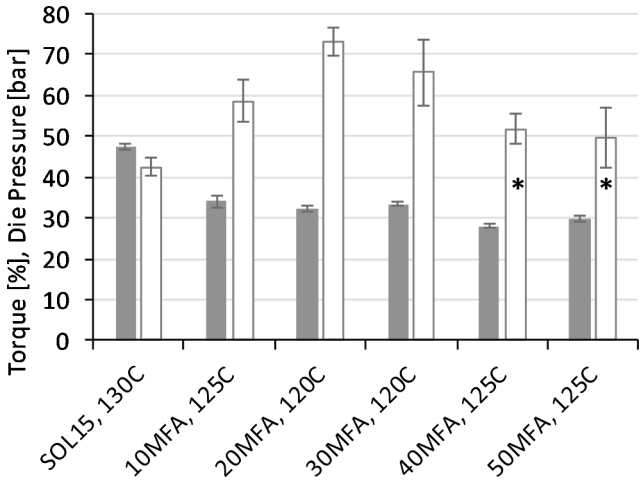

Fig. 3. HME process data for extrusion of 0–50MFA at 50 rpm screw speed and 0.1 kg/h powder feed rate; % torque – grey bar (all significantly different), die pressure – white bar (*not significantly different), 0 and 50MFA data from (Prasad et al., 2020)).

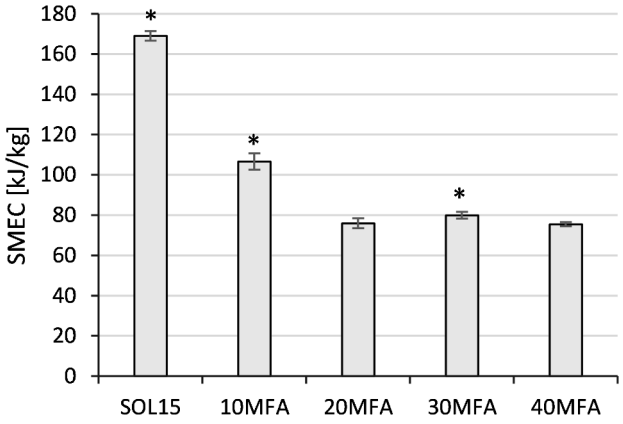

Fig. 4. Specific mechanical energy consumption (SMEC) for extrusion of 0 – 40MFA at 130 °C, screw speed 50 rpm, feed rate 0.1 kg/h.

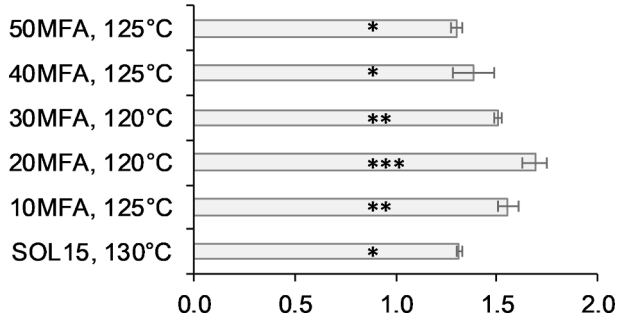

Fig. 5. Die swell ratio of 0−50MFA extrudates (0 and 50MFA data from (Prasad et al., 2020)). One-way ANOVA groupings that are significantly different are indicated with *, **, ***.

(SeethaLekshmi and Guru Row, 2012), exhibiting an endothermic transition of MFA form I to MFA form II at 172.8 °C and a melting endotherm of the latter at 233 °C (Fig. 7). PMs of MFA, Soluplus® and D-Sorbitol, showed thermal events relating to the Tg of the polymer (~66 °C), Sorbitol melt endotherm (100 °C), MFA phase transition to form II and melt endotherm for MFA II. With increasing drug loading, the MFA transition and melt endotherm shifted to higher temperatures

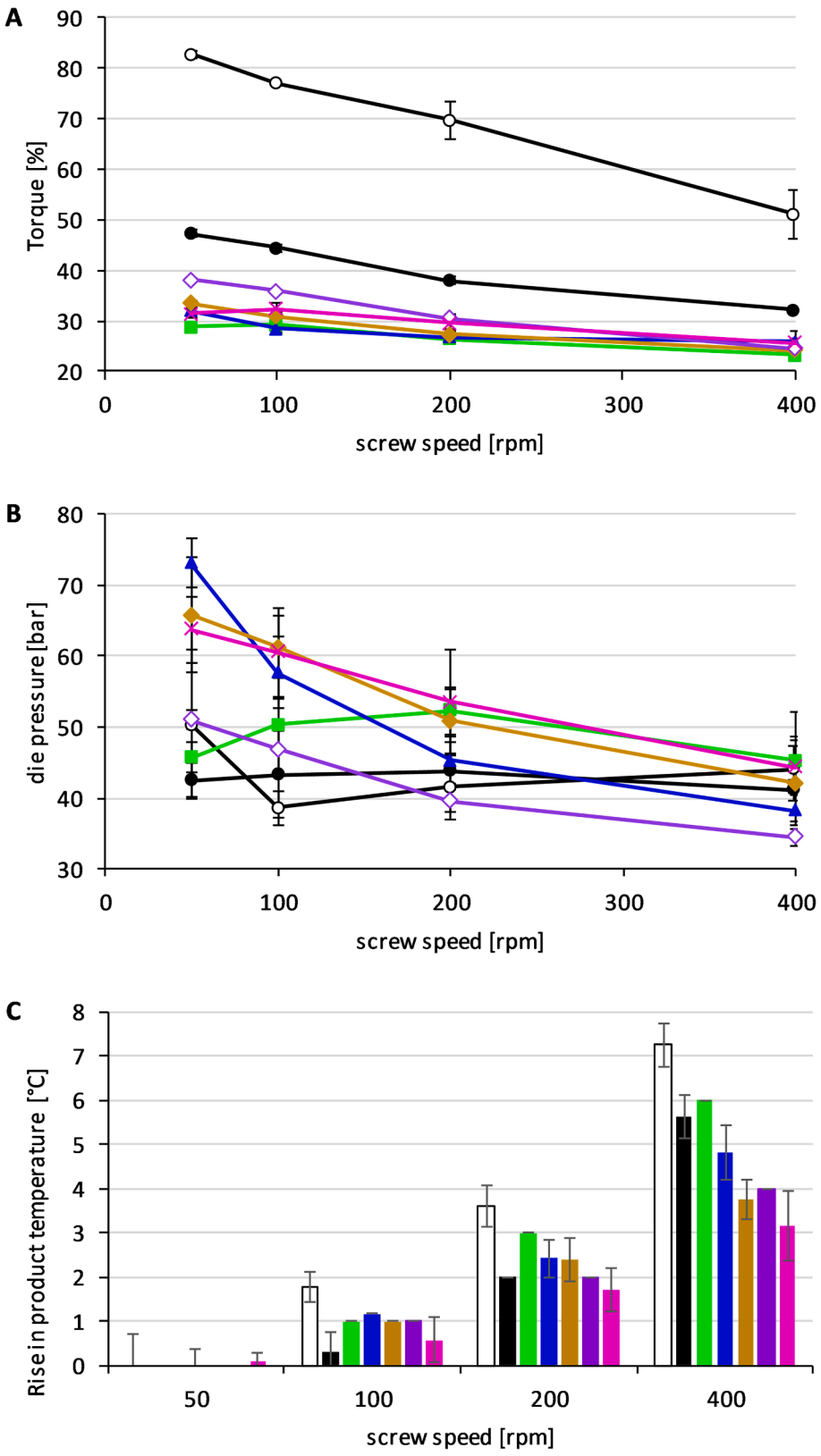

Fig. 6. Impact of screw speed on HME process parameters: (A) torque, (B) die pressure and (C) rise in product temperature. Soluplus® – black open circle/white bar, SOL15 – black filled circle/black bar, 10MFA – green square, 20MFA – blue triangle, 30MFA – brown filled diamond/bar, 40MFA – purple open diamond/bar, 50MFA – pink asterisk/bar.

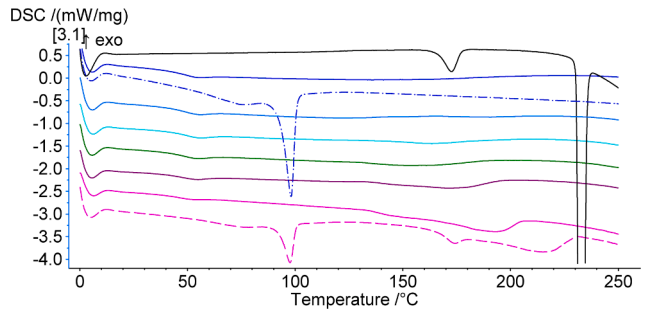

Fig. 7. Thermogram for heating cycle from 0 to 250 °C at 20 °C/min of physical mixtures (PM) and extrudate (EX) samples. From top to bottom: MFA powder - black; SOL15 EX – royal blue; SOL15 PM – royal blue, dash dotted line; 10MFA EX – blue; 20MFA EX - turquoise; 30MFA EX - green, 40MFA EX – purple, 50MFA EX – pink, 50MFA PM – pink, dashed line (n = 2).

(Figure S 1).

Thermal analysis of SOL15 and 50MFA have previously been reported (Prasad et al., 2020) and are included in the results for comparison. The polymer matrix only displayed a single Tg suggesting Sorbitol was fully dissolved in the polymer. Although the addition of Sorbitol to the polymer significantly decreased the Tg (Prasad et al., 2020), the addition of MFA to the system only showed minor additional Tg depression (~49.6–45.9 °C) (Figure S 2). MFA melt endotherms were observed for the 20 – 50 % w/w extrudates, indicative of the presence of crystalline MFA. 40 and 50 % w/w drug loaded extrudates showed an overlap of the transition and melt endotherm.

3.5. FTIR

The N-H stretching band of the amino group in MFA is associated with an intramolecular hydrogen bond with the carboxyl group (Abbas et al., 2017). In MFA form I polymorph, this hydrogen bond weaker than in form II and therefore displays this band at 3312 cm^{-1}, whereas the form II displays this at an energetically higher band at 3353 cm^{-1}. FTIR analysis confirmed the presence of MFA form I in the PMs, seen as an N-H stretch at 3307 cm^{-1} (Figure S 3). Extrudate samples showed a similar distinct N-H stretch for MFA form I at concentrations ≥ 30 % w/w MFA, confirming that MFA form I was retained under given process conditions. In contrast, 10MFA and 20MFA extrudates showed a weak and broad transmission peak in the N-H stretch region, indicative of the presence of amorphous MFA (Figure S 4).

3.6. XRPD

The presence of MFA form I (McConnell and Company, 1976) in the starting materials was confirmed by XRPD analysis, seen as a characteristic peak at ~ 6° 2-theta (Cunha et al., 2014; McConnell and Company, 1976) and four characteristic diffraction peaks between 14° – 16° 2-theta (McConnell and Company, 1976) (Fig. 8A b - f, Figure S 5). SOL15 PM was mainly amorphous in character with an indication of the presence of crystalline Sorbitol, seen as weak diffraction peaks at 11.8° and 18.8° 2-thea. SOL15 and 10MFA extrudates showed amorphous halos and lacked any sharp diffraction peaks, characteristic of amorphous materials (Fig. 8B a, b). 20MFA – 50MFA extrudates showed similar amorphous haloes but also diffraction patterns characteristic for MFA form I (McConnell and Company, 1976), suggesting Mefenamic acid form I was retained during HME processing.

3.7. Mechanical testing

The mechanical properties of SOL15 and 50MFA have previously been reported (Prasad et al., 2020) and are included in the results for comparison. The SOL15 filament presented as a stiff and strong filament, seen in a high flexural modulus (FM), high maximum stress (MS) and low associated strain values (Fig. 9). The flexural modulus, or elastic stiffness of the filaments followed a U-shape trend in relation to MFA composition (Fig. 9A). The decrease in FM at low drug loadings, was indicative of a plasticising effect of MFA reaching a minimum with 20 % w/w drug loading. This was followed by an increase in elastic stiffness at MFA concentrations ≥ 30 % w/w. One-way ANOVA test with Tukey pairwise comparison method showed two significantly different groupings with high (0, 40, 50 % w/w) and low (10, 20, 30 % w/w) elastic stiffness (Table S 5). A decrease in filament strength (MS) was also observed with increasing drug loadings (Fig. 9B, Table S 6). The lowest strength values were associated with API loadings ≥ 30% w/w. Strain values associated with the maximum stress showed three significantly different groupings compared to polymer matrix only: 1) polymer matrix only, 2) increase in strain at MS with 10 and 20 % w/w drug loading, 3) reduction in strain for 30 % w/w drug loading and 4) low strain values for 40 and 50 % w/w drug loading (Fig. 9C, Table S 7). The

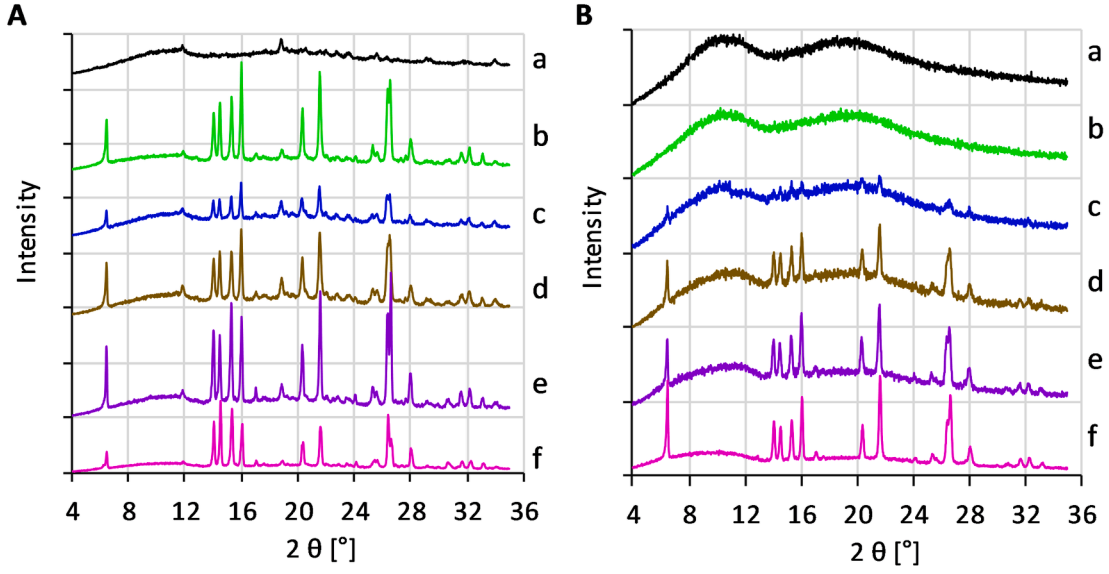

Fig. 8. XRPD data of 0 – 50MFA. Intensity versus 2-theta (θ): (A) Physical Mixtures and (B) Extrudates. From top to bottom: (a) SOL15 (black), (b) 10MFA (green), (c) 20MFA (blue), (d) 30MFA (brown), (e) 40MFA (purple), (f) 50MFA (pink).

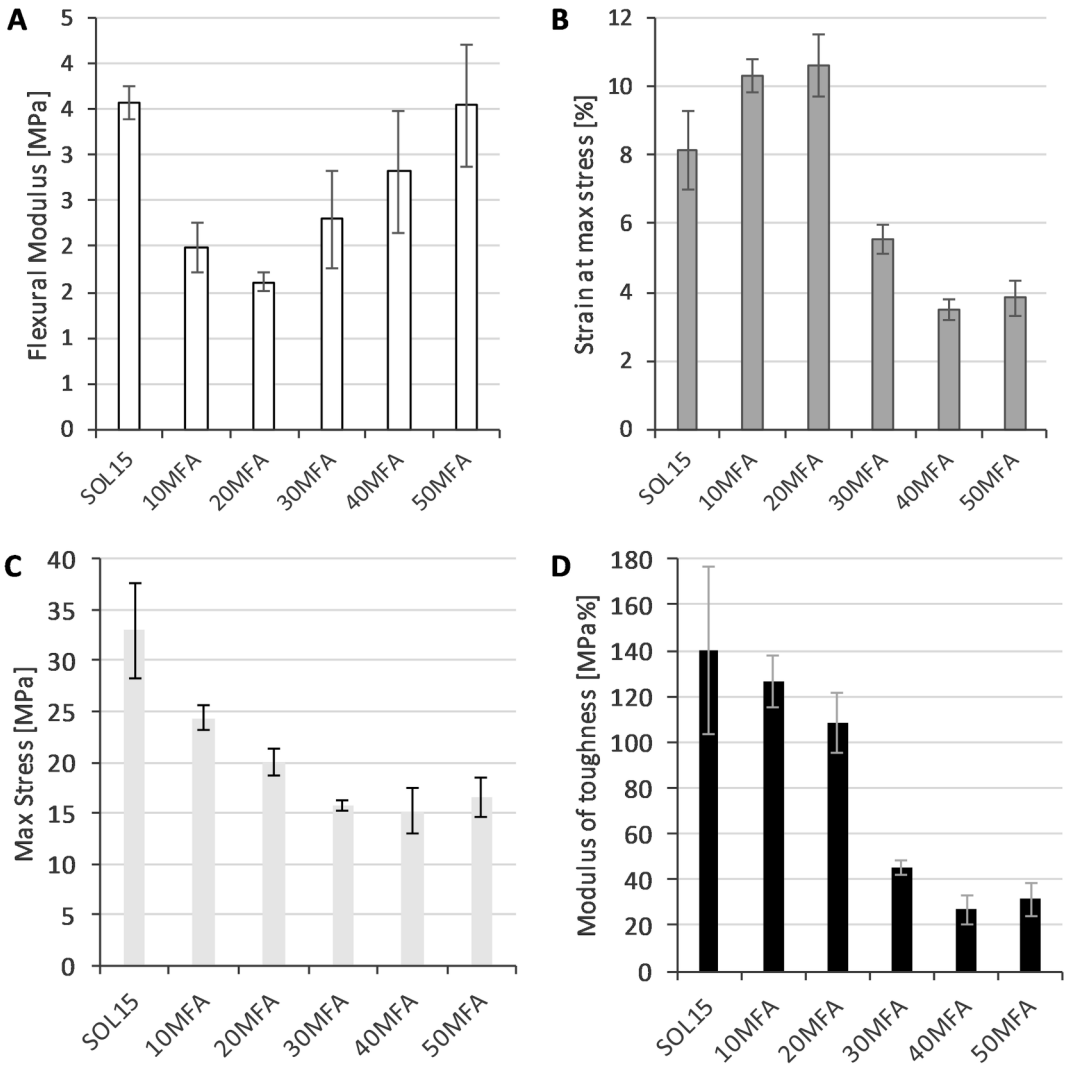

Fig. 9. Mechanical properties of extruded filaments (0 – 50MFA): (A) Flexural modulus (white), (B) Maximum stress (dark grey), (C) Strain at maximum stress (light grey) and (D) Modulus of toughness (black) (n = 5). (SOL15 and 50MFA from (Prasad et al., 2020)).

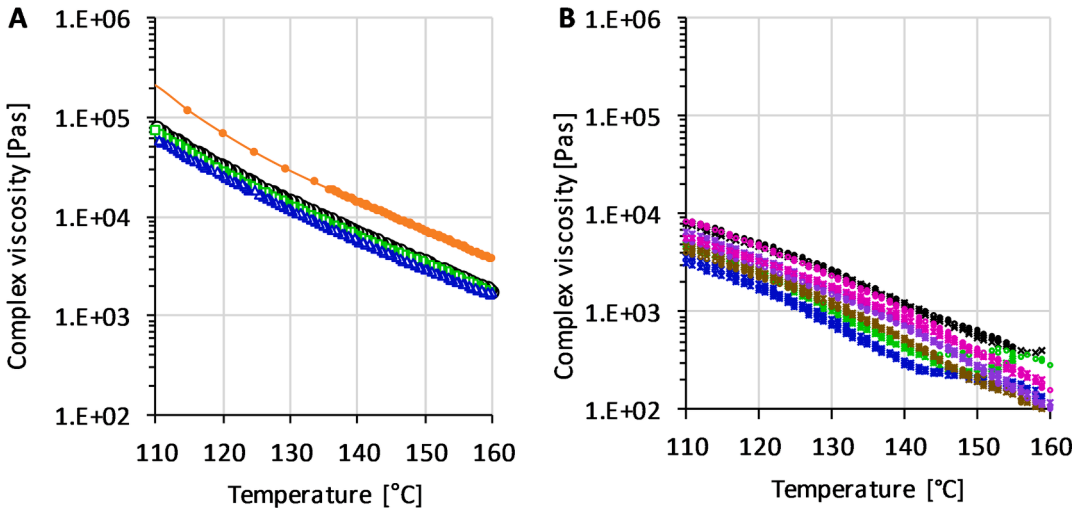

Fig. 10. Oscillatory temperature sweep: Complex viscosity versus temperature. (A) Physical Mixtures: Soluplus® – orange, filled circle, SOL15 PM – black, open circle, 10MFA PM – green, open square, 20MFA PM – blue, open triangle; (B) Extrudates: SOL15 EX – black, 10MFA EX – green, 20MFA EX – blue, 30MFA EX – brown, 40MFA EX – purple, 50MFA EX – pink (n = 2).

modulus of toughness (MoT) is calculated as the area under the curve at break and is representative of the energy required for product failure. Two significantly different groupings were observed: 0–20% w/w MFA showed high moduli of toughness, whereas 30 – 50 % w/w MFA showed significantly lower values (Fig. 9D, Table S 8).

3.8. Rheology – Extrudates

The complex viscosity of SOL15 and 10MFA – 50MFA formulations post processing was significantly lower (~14 fold) than the PMs, demonstrating the effect of the hot melt extrusion process on the polymer and API-polymer system, increasing polymer-plasticiser and polymer-plasticiser-API interactions.

The complex viscosity of SOL15 was higher than extrudates containing MFA. The addition of 10% MFA saw a significant vertical down shift of the complex viscosity – temperature curve, the plasticising effect of MFA on the polymer (Fig. 10B). Noisy data was observed for the 10MFA sample at temperatures above 145 °C. This coincided with the sample squishing out of the gap between the upper and lower plate in the rheometer. The sample did not flow out of the gap. Instead, the sample retained some level of structure, touching the outside of the upper plate in the measurement geometry. This may therefore have distorted measured data. A similar observation regarding the gap was made for the 20MFA extrudate. In addition, a further vertical down shift was observed for the complex viscosity - temperature curve. Demonstrating an additional plasticisation effect of MFA at higher loading in the polymer system. However, the vertical shift was not as large as the 0–10% w/w drug loading shift. 20MFA showed the lowest complex viscosity - temperature profile. Drug loadings ≥ 30% w/w saw an increase in complex viscosity, with drug loadings of 40 and 50% w/w showing the highest complex viscosity versus temperature profile.

For all MFA containing formulations (PM and EX), the viscous behaviour (G”>G’) dominated the system across the entire temperature range (data not shown), indicative of a system amenable to flow during processing steps.

Tan delta is the ratio of of viscous to elastic properties and is sensitive to structural changes in a sample. The SOL15 tan delta curve showed a faint peak or rather a ‘kink’ at 130 °C (Fig. 11). This tan delta peak temperature corresponded well with the lowest processing temperature of SOL15 on the 11 mm extruder (Fig. 3). With increasing drug loading, an increase in tan delta peak temperatures was observed (Fig. 11):

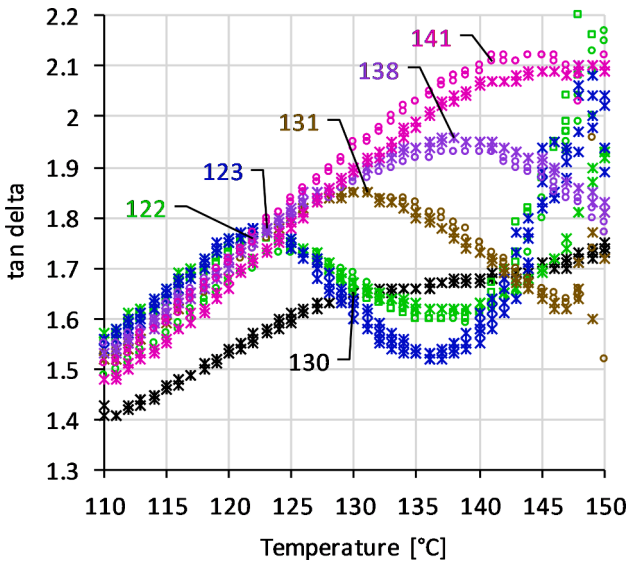

Fig. 11. Oscillatory temperature sweep: Tan delta versus temperature of 0 – 50MFA extrudates. SOL15 - black, 10MFA - green, 20MFA - blue, 30MFA – brown, 40MFA - purple, 50MFA – pink. (n = 2).

10MFA – 122 °C, 20MFA – 123 °C, 30MFA – 131 °C, 40MFA – 138 °C, 50MFA – 141 °C.

3.9. SEM

Cross sections (Fig. 12, Fig. 13) and outer surfaces (Fig. 14, Fig. 15) of extrudates were analysed by SEM analysis at x30 and x2000 magnification. SEM images of SOL15 and 50MFA extrudates have previously been published (Prasad et al., 2020) and were included in these results for comparison. The SOL15 extrudate presented as a uniform system on the cross section and the outer surface appeared smooth, which was in line with the thermal analysis and XRPD data showing a homogenous and fully amorphous system. The addition of MFA to the system resulted in the presence of small pores in the extrudate. These were predominantly observed across the cross section (Fig. 12, Fig. 13). At low drug loading of 10% w/w, pores were only visible at higher magnification (Fig. 13b). At 20 % drug loading a small number of larger pores were observed on the cross section (Fig. 12c, Fig. 13c). The number of larger sized pores increased substantially for the 30–50 % drug loaded filaments.

The lack of pores on the outer surface of extrudates may be due to MFA sublimation from the surface as the extrudate exits the hot HME die. This may be further facilitated through the low complex viscosity and predominantly viscous behaviour of the polymer matrix. The outer surface of SOL15, 10MFA, and 20MFA filaments seemed even and lacked pores, the 30 – 50 % drug loaded filaments looked coarser and indicated the presence of crystalline material. The crystalline domains were approximately ~ 5–10 μm in length for the highest drug loading, as previously reported (Prasad et al., 2020).

3.10. Performance screening – Inform

GI dissolution assays were performed with PMs and extrudates at physiologically relevant pH values of pH 2, 6.5 and 7.4. In addition, drug release was tested at pH 9.0, at which the quality control test for MFA capsules (USP37 Mefenamic acid capsules) is carried out. Data collection in each segment started once the target pH had been reached. PMs saw much lower drug release concentrations compared to their extruded counterparts (Fig. 16).

Mefenamic acid displayed low aqueous solubility across the physiologically relevant pH range. MFA is a weak acid with a pKa of 4.2. At pH 2 drug release is based on the release of the unionised, free acid form and was negligible for PMs (Fig. 16A) and extrudates (Fig. 16B).

A modest increase in maximum drug release at physiological pH values of pH 6.5 and pH 7.4 was observed for PMs, whereby 10MFA showed the highest maximum concentration of ~ 6.4 ug/mL at pH 7.4 compared to ~ 1.8 ug/mL for 50MFA PM. 10MFA extrudate reached significantly higher maximum concentrations across the pH range. Although the 20MFA – 50MFA extrudates showed marginally higher drug release than the PM, the release profiles were substantially lower than the 10MFA extrudate.

3.11. Drug release testing – USP37

Mefenamic acid capsules showed a relatively consistent drug release profile with a maximum variability of 7.5% (Fig. 17A). The average release reached 84.8 % ± 7.5 % at 45 min, failing to meet the immediate release requirements for Mefenamic acid (>85 % drug release at 45 mins).

The PM of 50MFA showed high (17.8%) variability in drug release between the 6 tested capsules (Fig. 17B). The average drug release at 45 mins was 86.6 % ± 6.1 %.

4. Discussion

The objective of this study was to develop an immediate release (IR),

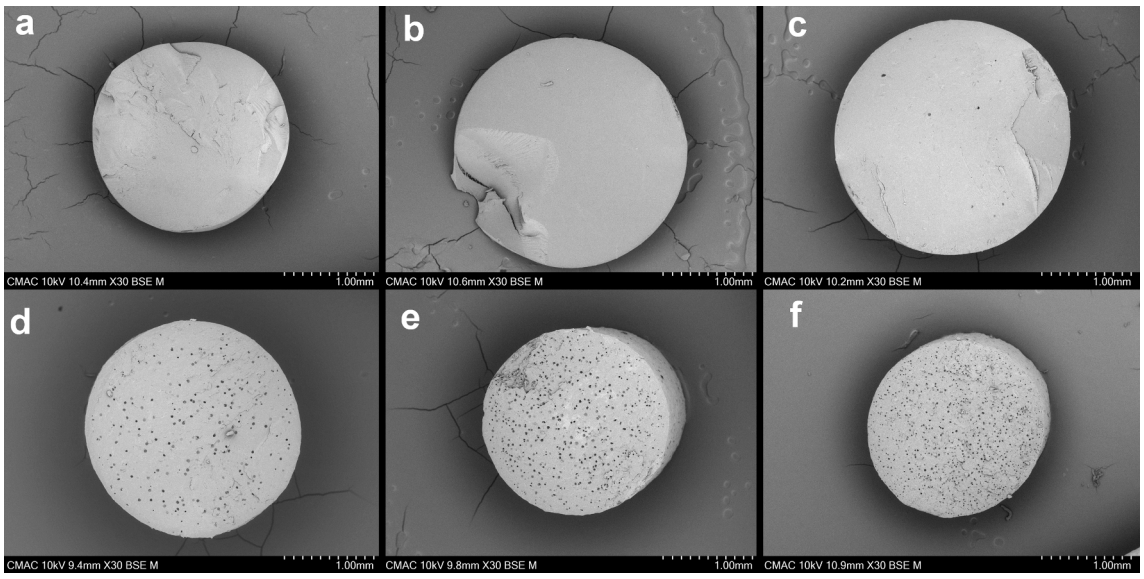

Fig. 12. SEM images of extrudate faces with x30 magnification: a - SOL15*, b – 10MFA, c – 20MFA, d – 30MFA, e – 40MFA, f – 50MFA* (*reprinted from Prasad et al., 2020, Copyright © 2020 American Pharmacists Association® with permission from Elsevier).

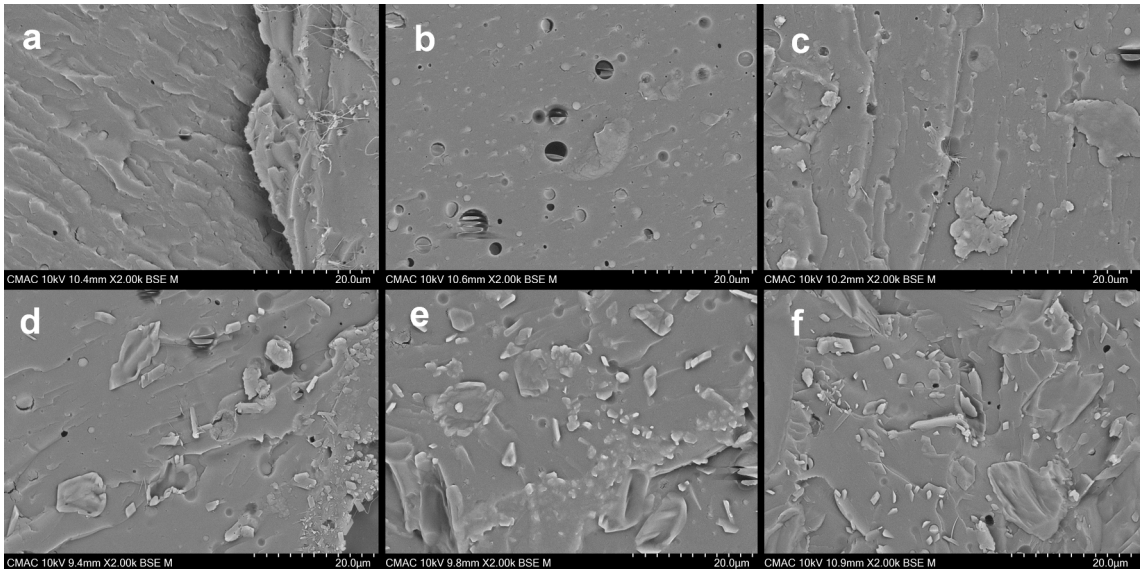

Fig. 13. SEM images of extrudate faces with x2000 magnification: a - SOL15*, b – 10MFA, c – 20MFA, d – 30MFA, e – 40MFA, f – 50MFA* (*reprinted from Prasad et al., 2020, Copyright © 2020 American Pharmacists Association® with permission from Elsevier).

crystalline solid dispersion (CSD) formulation of MFA by hot-melt-extrusion (HME) and assess the impact of drug loading on process parameters, physico-chemical properties and product performance.

A polyvinyl caprolactam–polyvinyl acetate–polyethylene glycol graft copolymer, Soluplus®, with 15% w/w D-Sorbitol was chosen due to the low HME processing temperatures (Kolter et al., 2012; Prasad et al., 2020). The viscoelastic properties of this plasticised polymer system (SOL15) at elevated temperatures and under shear (Prasad et al., 2020) are amenable to flow and may facilitate post processing steps such as 3D printing and/or injection moulding.

Predictive approaches for drug-polymer miscibility, e.g., the Hansen Solubility Parameters, aid the formulation development and selection of miscible API-polymer combinations. The resulting miscible combinations may exhibit lower levels of internally stored energy, resulting in longer stability of these extrudates. However, these do not predict the maximum solubility, or critical API concentration, in a given system. Such information would be useful, as the maximum solubility can vary for different API-polymer combinations (Bordos et al., 2019; Ekblad, 2018; Gupta et al., 2015; Solanki et al., 2018), resulting in different process- and product behaviour as reported in this study. The structured development program based on screening assays applied in this study, offered advantages over predictive models.

Standard practice to identify suitable process temperatures for initial HME trials is often based on Tg values of the polymer plus 20 – 40 °C (Kulkarni et al., 2018), resulting in a large temperature range to be investigated, requiring larger quantities of material for process development. In this study, the evaluation of rheological screening assays of PMs provided a more detailed insight into the polymer melt behaviour in the extruder, allowing for a more accurate estimation of suitable process conditions and low material usage. The small discrepancy (5 – 10 °C) between the predicted and actual lowest process temperatures was possibly due to the mechanical mixing in the extruder facilitating some

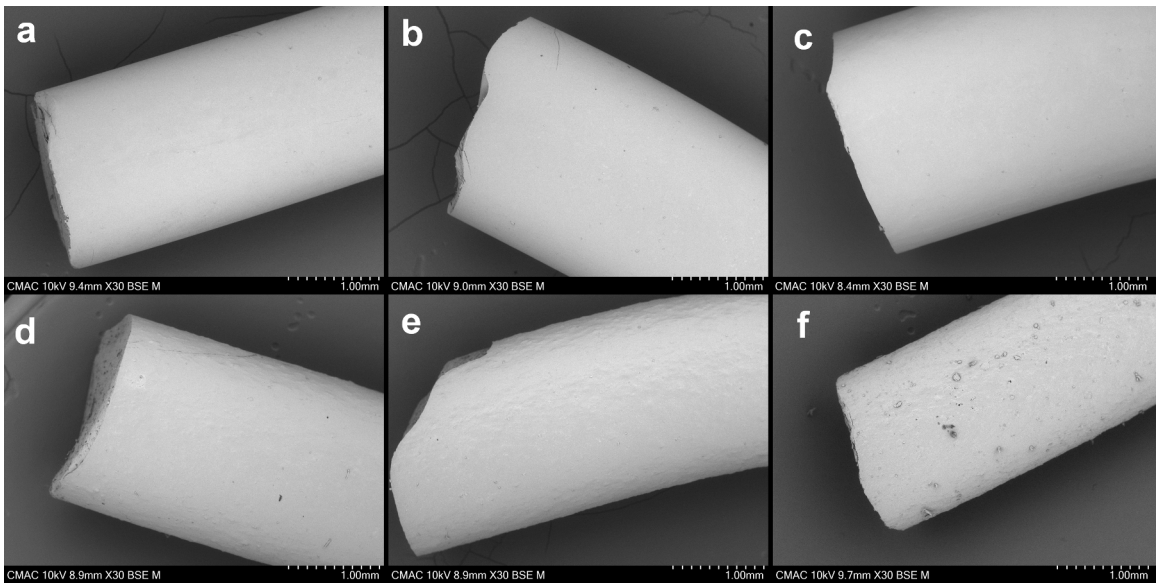

Fig. 14. SEM images of extrudate outer surface with x30 magnification: a - SOL15*, b – 10MFA, c – 20MFA, d – 30MFA, e – 40MFA, f – 50MFA* (*reprinted from Prasad et al., 2020, Copyright © 2020 American Pharmacists Association® with permission from Elsevier).

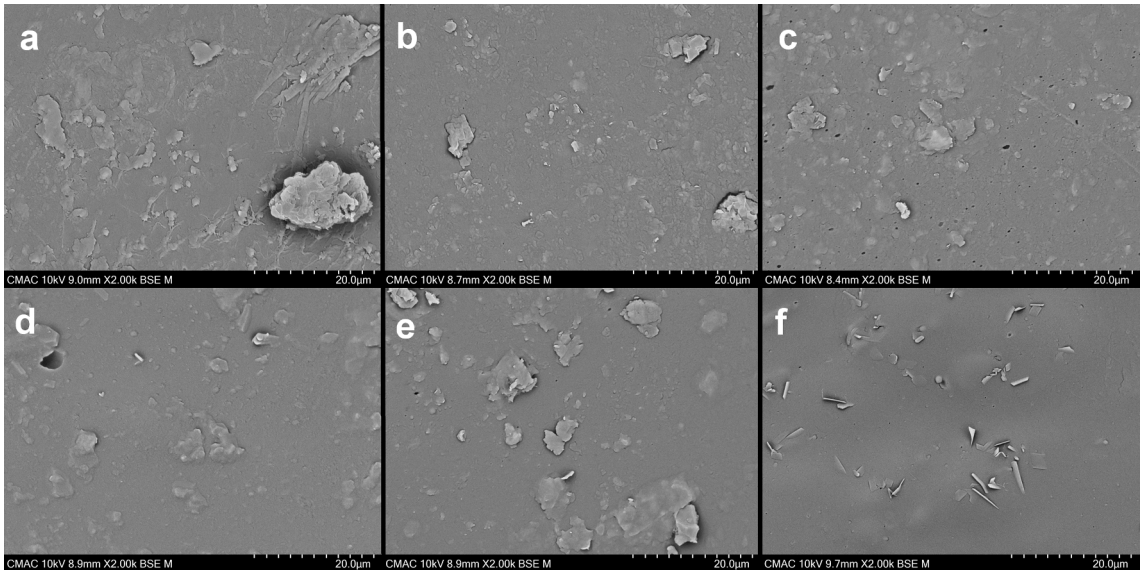

Fig. 15. SEM images of extrudate outer surface with x2000 magnification: a - SOL15*, b – 10MFA, c – 20MFA, d – 30MFA, e – 40MFA, f – 50MFA* (*reprinted from Prasad et al., 2020, Copyright © 2020 American Pharmacists Association® with permission from Elsevier).

level of MFA dissolution in the polymer matrix during the HME process (Fig. 3, Fig. 1). This is not unusual, solid dispersions prepared by vacuum compression moulding, lacking a typical HME shear and mixing profile, did not facilitate full drug dissolution at the same drug loading and processing temperatures (Ekblad, 2018) compared to an HME process.

At drug loadings in excess of 30 % w/w, the rheological screening method showed poor repeatability, highlighting the limitations of this assay. This was in agreement with other studies where rheological assessments guided the selection of HME processing conditions. These rheological screening studies on PMs were successful for APIs which dissolved in the carrier matrix (Aho et al., 2015; Gupta et al., 2016; Yang et al., 2016), but failed with high concentrations of API's exhibiting low solubility in the polymer matrix (Prasad et al., 2020). Despite the limitations at high drug loadings, the presence of MFA particles in the system still provided information on the viscoelastic properties (Fig. 1) for a CSD formulation linked to the HME process, e.g., reduced die swell in the presence of MFA particles. Increasing presence of MFA particles resulted in reduced die swell for MFA concentrations exceeding 20% (Fig. 5). Similar observations of polymer melts displaying decreased levels of elasticity, have been associated with the presence of undissolved fillers in these polymer melts (Barnes, 2003; Kalantar Mehrjerdi et al., 2020). This is in contrast to the shear induced increase in elastic behaviour that has previously been reported for the polymer only system (Prasad et al., 2020) and may also be due to a dilution effect of the polymer/drug liquid versus free solid at higher drug loadings.

Three groupings of process- and product behaviour of this API-polymer matrix system were identified during HME processing and product analysis for this range of formulations. These groupings were slightly different for the HME process and the cooled product / filament. (Table 3): in the HME process, at elevated temperatures, the polymer is in a semisolid/liquid state, opposed to the solid state of the cooled down filament.

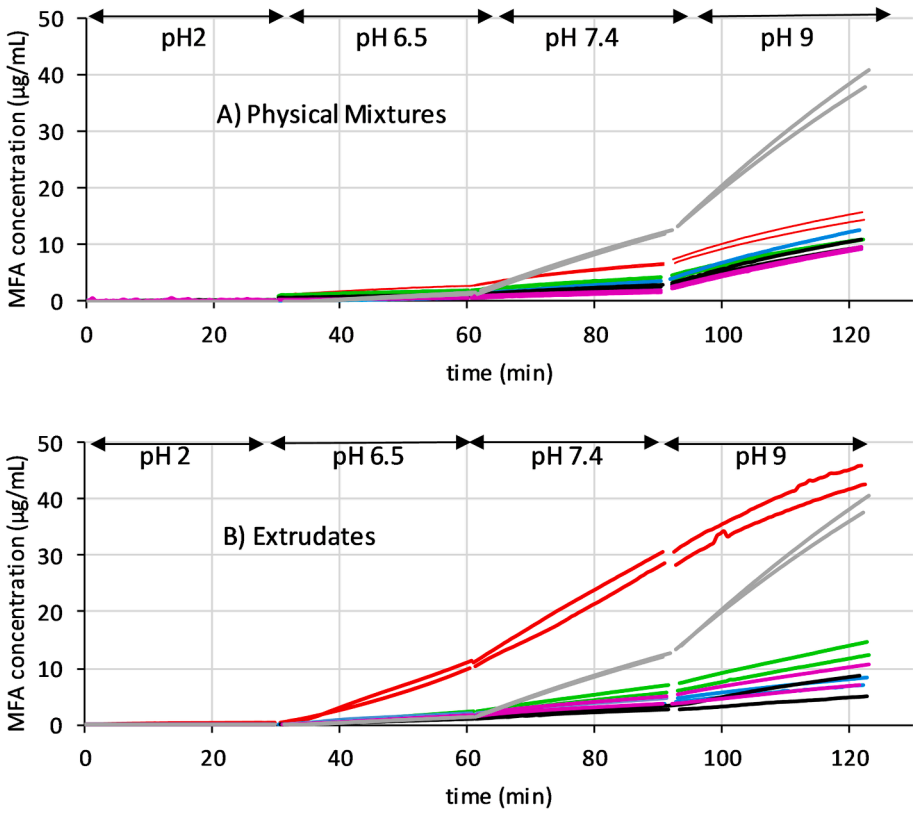

Fig. 16. Inform GI dissolution assay for A) Physical Mixtures and B) Extrudates of 10 – 40 % w/w MFA extrudates: 30 min per pH sector at pH 2, pH 6.8, pH 7.4 and pH 9 (25 °C). 10MFA-red, 20MFA – green, 30MFA – blue, 40MFA – black, 50MFA – pink, grey – MFA powder (Sigma) (n = 2).

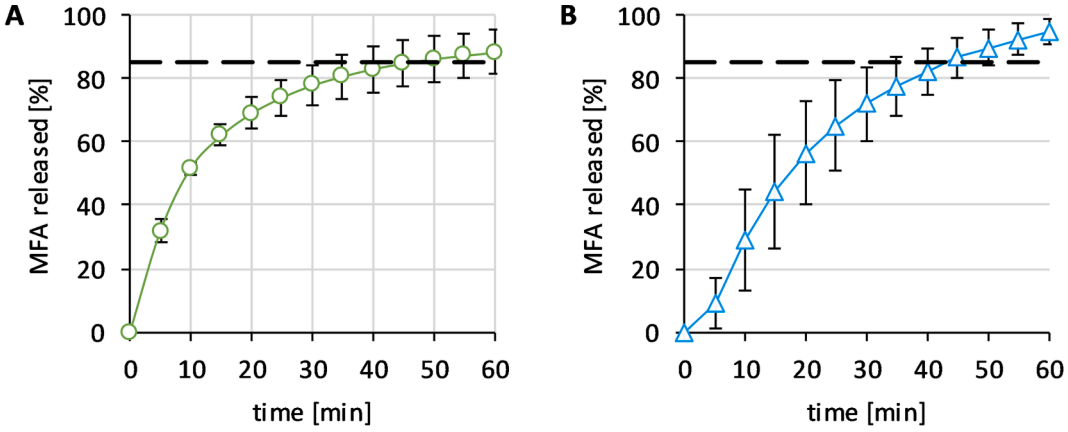

Fig. 17. USP II Dissolution test according to USP37 Mefenamic acid capsule: A) MFA powder only (Sigma) in capsules (green, open circle), B) 50MFA PM (physical mixture) in capsules (blue, open triangle) (n = 6).

Table 3
Groupings for process and product data.

Category	sub-saturated	saturated	super-saturated
Solid state	AMORPHOUS	mainly AMORPHOUS + crystalline	mainly CRYSTALLINE + amorphous
Process	10% w/w	20/30% w/w	40/50% w/w
Product	10% w/w	20% w/w	30–50% w/w

The behaviour of the formulation in the process and product was related to the ratio of drug loading to maximum solubility of the API in the polymer matrix and was grouped into three broad categories of: a) sub-saturated, b) saturated, and c) super-saturated systems (Table 3). For these three categories, the behaviour of the sub-saturated system was mainly dominated by the polymer with the system exhibiting a coherent polymer network (Fig. 9) of amorphous character (Fig. 8). The saturated system comprised API concentrations close to the maximum solubility of API in polymer matrix. This system was similar to the sub-saturated system with respect to the predominantly amorphous character, but also contained crystalline material (Fig. 8) that did not disrupt the (coherent and stable) polymer network. The super-saturated system exhibited crystalline, API rich, domains (Fig. 8) which disrupted the polymer network (Fig. 9).

Both, the process and product related data, indicated that the maximum solubility of MFA in the polymer matrix was between 10 and 20 % w/w. For the HME process in this study, the maximum solubility

was most clearly seen in the change in SMEC related to drug loading, as well as the lowest process temperature (Fig. 3, Fig. 4). Whereas the complex viscosity measurements of the drug product gave the clearest indication of the maximum solubility (Fig. 10). The elastic stiffness (Fig. 9) of the product was also highly sensitive to the solid state of the drug in the polymer matrix. However, these measurements were also impacted by the presence of pores in the system and may require careful interpretation.

Similar (three) groupings for the behaviour of a Soluplus® system have been reported, with the medium drug loaded formulation extruding at lower temperatures than formulations with low and high drug (Itraconazole) content (Solanki et al., 2018). In addition, three groupings for process and product analysis have been reported for an API-polymer system comprising 0–50% w/w PCM in HPMC (Affinisol™ 15LV) (Prasad et al., 2019). The maximum solubility can vary for different API-polymer combinations (Bordos et al., 2019; Ekblad, 2018; Gupta et al., 2015; Parikh et al., 2015; Solanki et al., 2018). In the case of Soluplus®, maximum solubilities of APIs have been reported as varying from 10 % w/w for Celecoxib (Ekblad, 2018) to 30 % w/w for Naproxen (Ekblad, 2018), Itraconazole (Parikh et al., 2015; Solanki et al., 2018) and Carbamazepine (Gupta et al., 2015).

Further studies are required to confirm the exact maximum solubility of MFA in this polymer matrix. Recently, (THz) Raman spectroscopy was successfully employed as an in-line process analytical tool to determine the saturated solubility of crystalline API in polymeric matrices directly during hot melt extrusion (Bordos et al., 2019). A similar approach to assess the MFA-Sorbitol-Soluplus® system would be useful in determining an equilibrium solubility phase diagram and is currently under investigation in our laboratories.

Dissolution of MFA, as a weak, lipophilic (logP 5.1 (Information, 2020)) acid, was primarily driven by pH, where deprotonation of the carboxylic acid group at high pH (pH 9) facilitated drug dissolution. Consequently, only a modest difference between 20MFA – 50MFA PMs and extruded formulations was observed for drug dissolution at physiologically relevant pHs (Fig. 16).

It may have also been impacted by the sample presentation of the powdered samples in the Sirius Inform system. The Sirius Inform system is a dissolution screening platform to assess and compare dissolution performance of formulations. Due to the assay setup and the small dissolution volume of 40 mL, it was not possible to add samples in hard gelatine capsules. Instead, PM samples were added as free powder, allowing the powder to easily disperse within the medium. Under this setup, the complex function of rates of different processes seen for dissolution of drugs from capsules, such as solution of the gelatine shell, penetration of water into the powder mass and de-aggregation of the powder mass (Shinkuma et al., 1984) were not observed. Instead, drug dissolution may have been primarily influenced by dissolution properties of powder particles and to a lesser extent the presence of excipients.

Amorphization of MFA in the 10MFA formulation (Fig. 7, Fig. 8), also exhibiting the highest excipient to drug ratio, resulted in improved dissolution. This was in stark contrast to the performance of higher drug loadings, even at physiologically relevant pHs (Fig. 16). In amorphous solid dispersions, the particle size is reduced to the absolute minimum and the internal free energy of the system is increased aiding drug dissolution. Similar effects of polymer to drug ratio on release profiles of amorphous solid dispersions of MFA in Eudragit and Soluplus® have previously been reported (Darwich, 2015). The differences in dissolution profiles were even more pronounced at pH 9, the USP dissolution test conditions. This behaviour for the formulation with the highest excipient to drug ratio, was in line with reports that drug dissolution mechanisms at low API concentrations are polymer controlled, whereas API controlled at high API concentrations (Craig, 2002; Karavas et al., 2007).

In order to understand how the assessment of the formulations in the Inform setup translated to the pharmacopeial USP I test, MFA powder only and the physical mixture of 50MFA were assessed. The pharmacopeial test was performed at high pH (pH 9) and in the presence of a high concentration (2 %) of surfactant (SDS), both of which significantly increase the dissolution of MFA. In this instance a slightly larger dissolution volume (of 1000 mL) was used to allow for inline UV quantification, which may have slightly increased drug release over time. A pharmacopeial test serves as a quality control test of manufactured dose forms and forms the basis for product release criteria. In this study, hand filled capsules containing Mefenamic acid powder only (Sigma) and a PM of 50MFA were tested under the same conditions. Although both tests failed to meet 85% drug release at 45 min, drug release was slightly higher for the PM, demonstrating excipients in the capsule aiding the dissolution process. However, the PM showed high levels of variability in the dissolution assay (17.8 % at 15 mins, Fig. 17, Table 4). Similar observations were made in a previous study where a commercially available MFA capsule (250 mg, Pharmavit Ltd) showed comparable high levels of variability (17.0 % at 20 mins) (Prasad et al., 2020); highlighting the impact of sample presentation (powder filled capsule versus free powder) in a dissolution test setup and the complex functions of dissolution rates from powder filled capsules reported by Shinkuma et al (Shinkuma et al., 1984). In contrast, presentation of 50MFA as a CSD formulation filled into capsules showed not only improved consistency in drug release (max variability 5.9 % at 20 mins), but also achieved complete dissolution (>85% at 45 mins) (Prasad et al., 2020). Sample presentation in the Inform assay setup did not accommodate for these occurrences/observations. CSD formulations of MFA primarily improved performance by improving the consistency of dissolution and to a lesser degree dissolution rates, whereas an ASD formulation improved both. Based on the therapeutic dose of MFA acid (250 mg), high drug loading was sought to minimise size and mass of the dose form, rendering low drug loaded formulations not feasible for product development.

Further investigations, such as the impact of available surface area, the presence of dissolved/undissolved excipient in the dissolution medium, buffer composition etc are desired to further the understanding of the product performance of these formulations.

5. Conclusion

The application of rheology screening to the HME process development facilitated detection of appropriate processing conditions (process temperature, screw speed), needing less material. Although this material sparing approach to HME process development was successful in this instance, it also emphasises the limitations of these screening assays for APIs with low solubility in a polymer.

Table 4
Comparison of product performance of different formulations: MFA powder only, 50MFA-SOL15 PM, Mefenamic acid 250 mg capsule (Pharmavit Ltd, Batch 4348) and 50MFA-SOL15 extrudate (pelletised).

Product tested	% Drug release at 45 mins	Max Variability (%), at time	% drug release >85% at time (if different from 45 mins)	Reference
MFA powder only (Sigma) (size 0 hard gelatine capsules)	84.8 % ± 7.5 %	7.5 % 45 mins	n/a	This study
50MFA PM (size 0 hard gelatine capsules)	86.6 % ± 6.1 %.	17.8 % 15 mins	92.5 % ± 4.8 % at 55 mins	This study
Mefenamic acid 250 mg capsule, Pharmavit Ltd, Batch 4348	91.3 % ± 4.7 %	17.0 % 20 mins	n/a	Prasad et al., 2020
50MFA extrudate (pelletised, size 0 hard gelatine capsules)	96.0 % ± 4.1 %	5.9 % 20 mins	93.5 % ± 4.3 % at 35 mins	Prasad et al., 2020

The targeted CSD formulation containing the stable polymorphic form I was successfully obtained for formulations containing 20 – 40 % w/w drug, whereas the 10MFA formulation presented as an ASD. The behaviour of the formulation in the process and product was related to the ratio of drug loading to maximum solubility of the API in the polymer matrix and was grouped into three broad categories of: a) sub-saturated, b) saturated, and c) super-saturated systems. The presentation of the formulation as a CSD primarily improved the consistency of drug release (Prasad et al., 2020). Despite superior product performance of an ASD formulation, achieving a therapeutic dose with such low drug loading would not be feasible. Additional studies into the critical concentration for amorphous material and product stability need to be carried out.

This study illustrates the impact of drug loading on process and product characteristics and how a better understanding of maximum API solubility in a given polymer system can improve targeted formulation development.

This work forms part of the broader aim of the EPSRC Future Manufacturing Research HUB at CMAC. The project aims to implement integrated continuous, laboratory scale manufacturing platforms by the means of crystal engineering of a model drug (MFA), coupled with polymer processing steps to deliver enhanced physical properties for biopharmaceutics performance. It forms the basis for future work within the HUB, how coupling crystal engineering with polymer processing may facilitate future performance-based design and continuous manufacture of structured particulate products (Prasad et al., 2020).

Data statement

All data underpinning this publication are openly available from the University of Strathclyde KnowledgeBase at: https://doi.org/10.15129/8597108f-6daa-43e1-8d2d-796b97c36f3a.

Credit authorship contribution statement

Elke Prasad: Project administration, Investigation, Validation, Visualization, Formal analysis, Data curation, Writing – original draft. **John Robertson:** Conceptualization, Project administration, Supervision, Writing - review. **Gavin W. Halbert:** Conceptualization, Supervision, Writing - review.

Declaration of Competing Interest

The authors declare that they have no known competing financial interests or personal relationships that could have appeared to influence the work reported in this paper.

Acknowledgements

The authors would like to acknowledge that this work was carried out in the CMAC National Facility supported by the EPSRC (Grant ref EP/P006965/1) and by UKRPIF (UK Research Partnership Fund) award from the Higher Education Funding Council for England (HEFCE) (Grant ref HH13054). G. W. Halbert is funded by Cancer Research UK (C149/A20496). We would like to thank the National Facility team for their support in this project. We would also like to thank BASF for the donation of Soluplus® polymer.

Appendix A. Supplementary material

Supplementary data to this article can be found online at https://doi.org/10.1016/j.ijpharm.2022.121505.

References

Abbas, N., Oswald, I., Pulham, C., 2017. Accessing mefenamic acid form II through high-pressure recrystallisation. Pharmaceutics 9 (4), 16. https://doi.org/10.3390/pharmaceutics9020016.

Abdul Mudalip, S.K., Abu Bakar, M.R., Jamal, P., Adam, F., 2013. Solubility and dissolution thermodynamic data of mefenamic acid crystals in different classes of organic solvents. J. Chem. Eng. Data 58 (12), 3447–3452. https://doi.org/10.1021/je400714f.

Aho, J., Boetker, J.P., Baldursdottir, S., Rantanen, J., 2015. Rheology as a tool for evaluation of melt processability of innovative dosage forms. Int. J. Pharm. 494 (2), 623–642. https://doi.org/10.1016/j.ijpharm.2015.02.009.

Alshehri, S.M., Park, J.B., Alsulays, B.B., Tiwari, R.V., Almutairy, B., Alshetaili, A.S., Morott, J., Shah, S., Kulkarni, V., Majumdar, S., Martin, S.T., Mishra, S., Wang, L., Repka, M.A., 2015. Mefenamic acid taste-masked oral disintegrating tablets with enhanced solubility via molecular interaction produced by hot melt extrusion technology. J. Drug. Deliv. Sci. Technol. 27, 18–27. https://doi.org/10.1016/j.jddst.2015.03.003.

Andrews, G.P., Zhai, H., Tipping, S., Jones, D.S., 2009. Characterisation of the thermal, spectroscopic and drug dissolution properties of mefenamic acid and polyoxyethylene-polyoxypropylene solid dispersions. J. Pharm. Sci. 98 (12), 4545–4556. https://doi.org/10.1002/jps.21752.

Barnes, H.A., 2003. A review of the rheology of filled viscoelastic systems. Rheol. Rev. 1–36.

Bordos, E., Islam, M.T., Florence, A.J., Halbert, G.W., Robertson, J., 2019. Use of terahertz-Raman spectroscopy to determine solubility of the crystalline active pharmaceutical ingredient in polymeric matrices during hot melt extrusion. Mol. Pharm. 16 (10), 4361–4371. https://doi.org/10.1021/acs.molpharmaceut.9b0070310.1021/acs.molpharmaceut.9b00703.s001.

Brittain, H.G., 2016. Polymorphism in Pharmaceutical Solids. informa healthcare USA, Inc, New York.

Butler, J.M., Dressman, J.B., 2010. The developability classification system: application of biopharmaceutics concepts to formulation development. J. Pharm. Sci. 99 (12), 4940–4954. https://doi.org/10.1002/jps.22217.

Craig, D.Q.M., 2002. The mechanisms of drug release from solid dispersions in water-soluble polymers. Int. J. Pharm. 231 (2), 131–144.

Cunha, V.R.R., Izumi, C.M.S., Petersen, P.A.D., Magalhães, A., Temperini, M.L.A., Petrilli, H.M., Constantino, V.R.L., 2014. Mefenamic acid anti-inflammatory drug: probing its polymorphs by vibrational (IR and Raman) and solid-state NMR spectroscopies. J. Phys. Chem. B 118 (16), 4333–4344. https://doi.org/10.1021/jp500988k.

Darwich, M., 2015. Solubility/Bioavailability Enhancement and Modified Release Formulations of Poorly Water-Soluble Drugs. Freie Universität Berlin, Berlin. PhD.

Derle, D.V., Bele, M., Kasliwal, N., 2008. In vitro and in vivo evaluation of mefenamic acid and its complexes with beta-cyclodextrin and HP-beta-cyclodextrin. Asian J. Pharmac. 2, 30–34. https://doi.org/10.22377/ajp.v2i1.167.

Ekblad, N., 2018. Melt Processability of Amorphous Solid Dispersions during Hot-melt Extrusion. Screening Using Vacuum Compression Moulding and Evaluation by Rheology and Solid-state Analysis. UiT The Arctic University of Norway, Tromso. Master thesis.

Gravestock, T., Box, K., Comer, J., Frake, E., Judge, S., Ruiz, R., 2011. The "GI dissolution" method: a low volume, in vitro apparatus for assessing the dissolution/precipitation behaviour of an active pharmaceutical ingredient under biorelevant conditions. Anal. Methods 3, 560–567. https://doi.org/10.1039/C0AY00434K.

Gupta, S.S., Parikh, T., Meena, A.K., Mahajan, N., Vitez, I., Serajuddin, A.T.M., 2015. Effect of carbamazepine on viscoelastic properties and hot melt extrudability of Soluplus®. Int. J. Pharm. 478 (1), 232–239. https://doi.org/10.1016/j.ijpharm.2014.11.025.

Gupta, S.S., Solanki, N., Serajuddin, A.T.M., 2016. Investigation of thermal and viscoelastic properties of polymers relevant to hot melt extrusion, IV: Affinisol HPMC HME polymers. AAPS PharmSciTech 17 (1), 148–157. https://doi.org/10.1208/s12249-015-0426-6.

Gursoy, R.N., Benita, S., 2004. Self-emulsifying drug delivery systems (SEDDS) for improved oral delivery of lipophilic drugs. Biomed. Pharmacother. 58 (3), 173–182. https://doi.org/10.1016/j.biopha.2004.02.001.

Hummel, D., Buchmann, S., 2000. Influence of mefenamic acid particle size on dissolution and bioavailability of tablets. Pharmazeutische Industrie 62, 452–456.

Information, N.C.f.B., 2020. PubChem Compound Summary for CID 4044, Mefenamic acid. https://pubchem.ncbi.nlm.nih.gov/compound/Mefenamic-acid#:~:text=Mefenamic%20acid%20has%20been%20detected,the%20mefenamic%20Acid%20action%20pathway (16 September 2020).

Kalantar Mehrjerdi, A., Bashir, T., Skrifvars, M., 2020. Melt rheology and extrudate swell properties of talc filled polyethylene compounds. e04060-e04060 Heliyon 6. https://doi.org/10.1016/j.heliyon.2020.e04060.

Karavas, E., Georgarakis, E., Sigalas, M.P., Avgoustakis, K., Bikiaris, D., 2007. Investigation of the release mechanism of a sparingly water-soluble drug from solid dispersions in hydrophilic carriers based on physical state of drug, particle size distribution and drug–polymer interactions. Eur. J. Pharm. Biopharm. 66 (3), 334–347. https://doi.org/10.1016/j.ejpb.2006.11.020.

Kolter, K., Karl, M., Gryczke, A., 2012. Hot-Melt Extrusion with BASF Pharma Polymers, 2nd Revised and Enlarged Edition ed. BASF The Chemical Company, Ludwigshafen, Germany.

Kulkarni, C., Kelly, A.L., Gough, T., Jadhav, V., Singh, K.K., Paradkar, A., 2018. Application of hot melt extrusion for improving bioavailability of artemisinin a thermolabile drug. Drug Dev. Ind. Pharm. 44 (2), 206–214. https://doi.org/10.1080/03639045.2017.1386200.

Kumar, M., Singh, D., Bedi, N., 2019. Mefenamic acid-loaded solid SMEDDS: an innovative aspect for dose reduction and improved pharmacodynamic profile. Ther. Deliv. 10 (1), 21–36. https://doi.org/10.4155/tde-2018-0053.

McConnell, J.F., Company, F.Z., 1976. N-(2,3-xylyl) anthranilic acid, C15H15NO2. Mefenamic acid. J. Cryst. Struct. Commun. 5, 861–864.

Nurhikmah, W., Sumirtapura, Y.C., Pamudji, J.S., 2016. Dissolution profile of mefenamic acid solid dosage forms in two compendial and biorelevant (FaSSIF) media. Sci. Pharm. 84, 181–190. https://doi.org/10.3797/scipharm.ISP.2015.09.

Owusu-Ababio, G., Ebube, N.K., Reams, R., Habib, M., 1998. Comparative dissolution studies for mefenamic acid-polyethylene glycol solid dispersion systems and tablets. Pharm. Dev. Technol. 3 (3), 405–412. https://doi.org/10.3109/10837459809009868.

Parikh, T., Gupta, S.S., Meena, A.K., Vitez, I., Mahajan, N., Serajuddin, A.T.M., 2015. Application of film-casting technique to investigate drug-polymer miscibility in solid dispersion and hot-melt extrudate. J. Pharm. Sci. 104 (7), 2142–2152. https://doi.org/10.1002/jps.24446.

Prasad, E., Islam, M.T., Goodwin, D.J., Megarry, A.J., Halbert, G.W., Florence, A.J., Robertson, J., 2019. Development of a hot-melt extrusion (HME) process to produce drug loaded Affinisol™ 15LV filaments for fused filament fabrication (FFF) 3D printing. Addit. Manuf. 29, 100776. https://doi.org/10.1016/j.addma.2019.06.027.

Prasad, E., Robertson, J., Halbert, G.W., 2020. Improving consistency for a Mefenamic acid immediate release formulation. J. Pharm. Sci. 109 (11), 3462–3470. https://doi.org/10.1016/j.xphs.2020.08.012.

Rao, K.R., Nagabhushanam, M.V., Chowdary, K.P., 2011. In vitro dissolution studies on solid dispersions of mefenamic acid. Indian J. Pharm. Sci. 73, 243–247. https://doi.org/10.4103/0250-474x.91575.

Romero, S., Escalera, B., Bustamante, P., 1999. Solubility behavior of polymorphs I and II of mefenamic acid in solvent mixtures. Int. J. Pharm. 178, 193–202. https://doi.org/10.1016/s0378-5173(98)00375-5.

SeethaLekshmi, S., Guru Row, T.N., 2012. Conformational polymorphism in a non-steroidal anti-inflammatory drug, mefenamic acid. Cryst. Growth Des. 12 (8), 4283–4289. https://doi.org/10.1021/cg300812v.

Shinkuma, D., Hamaguchi, T., Yamanaka, Y., Mizuno, N., 1984. Correlation between dissolution rate and bioavailability of different commercial mefenamic acid capsules. Int. J. Pharm. 21 (2), 187–200. https://doi.org/10.1016/0378-5173(84)90093-0.

Solanki, N., Gupta, S.S., Serajuddin, A.T.M., 2018. Rheological analysis of itraconazole-polymer mixtures to determine optimal melt extrusion temperature for development of amorphous solid dispersion. Eur. J. Pharm. Sci. 111, 482–491. https://doi.org/10.1016/j.ejps.2017.10.034.

Sriamornsak, P., Limmatvapirat, S., Piriyaprasarth, S., Mansukmanee, P., Huang, Z., 2015. A new self-emulsifying formulation of mefenamic acid with enhanced drug dissolution. Asian J. Pharm. Sci. 10 (2), 121–127. https://doi.org/10.1016/j.ajps.2014.10.003.

Surov, A.O., Terekhova, I.V., Bauer-Brandl, A., Perlovich, G.L., 2009. Thermodynamic and structural aspects of some fenamate molecular crystals. Cryst. Growth Des. 9 (7), 3265–3272. https://doi.org/10.1021/cg900002q.

Tambosi, G., Coelho, P.F., Luciano, S., Lenschow, I.C.S., Zétola, M., Stulzer, H.K., Pezzini, B.R., 2018. Challenges to improve the biopharmaceutical properties of poorly water-soluble drugs and the application of the solid dispersion technology. Matéria (Rio de Janeiro) 23.

Ullah, I., Baloch, M.K., Ullah, I., Mustaqeem, M., 2014. Enhancement in aqueous solubility of mefenamic acid using micellar solutions of various surfactants. J. Solut. Chem. 43 (8), 1360–1373. https://doi.org/10.1007/s10953-014-0217-9.

Vasconcelos, T., Sarmento, B., Costa, P., 2007. Solid dispersions as strategy to improve oral bioavailability of poor water soluble drugs. Drug Discov. Today 12 (23-24), 1068–1075. https://doi.org/10.1016/j.drudis.2007.09.005.

Yang, F., Su, Y., Zhang, J., DiNunzio, J., Leone, A., Huang, C., Brown, C.D., 2016. Rheology guided rational selection of processing temperature to prepare copovidone-nifedipine amorphous solid dispersions via Hot Melt Extrusion (HME). Mol. Pharm. 13 (10), 3494–3505. https://doi.org/10.1021/acs.molpharmaceut.6b0051610.1021/acs.molpharmaceut.6b00516.s001.

Zografi, G., Newman, A., 2017. Interrelationships between structure and the properties of amorphous solids of pharmaceutical interest. J. Pharm. Sci. 106 (1), 5–27. https://doi.org/10.1016/j.xphs.2016.05.001.